ANALYSIS OF MULTICHANNEL VIRTUAL SENSING ACTIVE NOISE CONTROL TO OVERCOME SPATIAL CORRELATION AND CAUSALITY CONSTRAINTS

Dongyuan Shi, Bhan Lam, and Woon-seng Gan

School of Electrical and Electronic Engineering, Nanyang Technological University, Singapore.

ABSTRACT

This paper revisits the virtual sensing active noise control (VS-ANC) technique and extends it to a general multichannel ANC (MCANC) implementation. A frequency domain analysis shows that the multichannel virtual sensing ANC (VS-MCANC) technique arrives at an optimal control filter to cancel the noise disturbance at the virtual locations and overcomes the spatial correlation and causality constraints between the physical microphone and the virtual microphone. A real-time control of broadband noise with a 4-channel VS-MCANC implemented in a test chamber validates its theoretical analysis and demonstrates its active control effectiveness.

Index Terms— Virtual Sensing, Active Noise Control.

1. INTRODUCTION

Active noise control (ANC), which creates a destructive anti-noise wave to attenuate noise, is increasingly prevalent (e.g., headsets, ventilation ducts, and window apertures) owing to its compact size, low cost and better low-frequency attenuation performance compared to passive techniques [1]. However, it is worth noting that the diameter of the 10 dB 'quiet zone' around the physical error microphone in conventional ANC is approximately one-tenth the acoustic wavelength, i.e., $\lambda/10$. Hence, traditional virtual sensing techniques were developed to move the quiet zone nearer to the desired locations in situations where the physical microphone placements are restricted (e.g., virtually placing the error microphone near the ear positions in an automobile headrest [2, 3]).

Many of the proposed virtual sensing ANC (VS-ANC) techniques [4] generate the quiet zone at the desired locations, using virtual microphones, which are usually farther downstream from the noise source than the physical error microphones [5]. There are generally two categories of VS-ANC techniques. The first category requires no offline training to obtain the system model and directly predicts the sound pressure level at the virtual microphone location based on some acoustical models [6, 7] or by extrapolation methods [8, 9]. However, the noise reduction performance of these approaches is highly sensitive to the accuracy of the model estimations, and they are only suitable for low-frequency tonal sound fields [6]. The second category requires a preliminary training stage to obtain a filter, which contains the system model from the physical to the virtual error microphone position or the information of the optimum noise control filter [10]. Subsequently, the pre-trained filter will assist the ANC system in obtaining the optimal control filter to mitigate the noise disturbance at the virtual microphone location [11].

Currently, some practical VS-ANC algorithms, which belong to the second category [12, 13], have been developed. By placing actual microphones at the virtual microphone locations, the remote microphone technique computes the observation filter from the power density of the physical and the virtual error signals [14, 15] or estimates the plant states by the Kalman filtering method [16]. Subsequently, the actual microphones at the virtual microphone location during the training stage is removed, and the observation filter or the plant states are utilized to predict the virtual error signal from the physical error signal [12]. However, the remote microphone technique requires a strong spatial correlation [17] and imposes a causality constraint [8] between the physical and virtual microphone positions. Hence, the positioning of the virtual and physical error microphones, usually through trial-and-error, is critical to the performance of the remote microphone technique. For instance, if the virtual microphone is closer to the secondary source than the physical error microphone, both the spatial correlation and causality constraints will be violated (i.e., the observation filter would become non-causal). To overcome these constraints, we revisit the virtual microphone control (VMC) system proposed in [18, 19, 20, 21] and extend it to a multichannel virtual sensing ANC (VS-MCANC)system.

2. THE VS-MCANC ALGORITHM

The VS-MCANC system consists of J references, K secondary sources, and M error microphones to cancel the disturbance from L primary sources at the N virtual microphones locations, as shown in Fig. 1. The VS-MCANC technique consists of two stages: the tuning stage, and the control stage. In the tuning stage, the sum-of-the-squared primary noise signals at the desired virtual error microphone locations (using actual microphones) are minimized. Once the control filter converges to their optimal solution, auxiliary

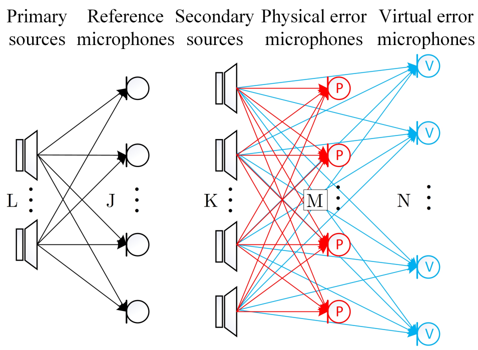

Fig. 1. Schematic of the VS-MCANC.

filters are trained to account for the differences between the physical and virtual paths (i.e., both the primary and secondary paths). In the control stage, the actual microphones at the virtual locations are removed. Both the physical error microphones and the auxiliary filters enable optimal noise control at the desired virtual microphone locations.

In the tuning stage, the output signal vector $\mathbf{y}(n)$ is given by

$$\mathbf{y}(n) = \mathbf{w}^T(n)\mathbf{x}(n), \tag{1}$$

where $\mathbf{w}(n)$ is the control filter matrix. The stacked reference vector $\mathbf{x}(n)$ is $[\mathbf{x}_1^T(n), \mathbf{x}_2^T(n), \cdots, \mathbf{x}_J^T(n)]^T$, and $\mathbf{x}_j(n)$ denotes the reference signal vector picked up by the jth reference microphone. Using the FxLMS algorithm, the update equation of the control filter from the jth input to the kth output is given by

$$\mathbf{w}_{kj}(n+1) = \mathbf{w}_{kj}(n) - \mu_1 \sum_{i=1}^{N} \mathbf{x}'_{v,jki}(n) e_{v,i}(n), \tag{2}$$

where $e_{v,i}(n)$ is the ith virtual error signal, and μ_1 denotes the step size in the tuning stage. The filtered reference $x'_{v,jki}(n)$ is the convolution of the jth reference signal $x_j(n)$ and the virtual secondary path estimate $\hat{g}_{v,ik}(n)$, which is from the kth secondary source to the ith virtual microphone.Once the control filter converges, the mth auxiliary filter stacked vector is obtained by

$$\begin{aligned}\mathbf{h}_m(n+1) =& \mathbf{h}_m(n) \\ &+ \mu_2 \left[e_{p,m}(n) - \mathbf{h}_m^T(n)\mathbf{x}(n)\right] \mathbf{x}(n),\end{aligned} \tag{3}$$

where $\mathbf{h}_m(n) = [\mathbf{h}_{m1}^T(n), \mathbf{h}_{m2}^T(n), \cdots, \mathbf{h}_{mJ}^T(n)]^T$ and $\mathbf{h}_{mj}(n)$ denotes the auxiliary filter from the jth reference to the mth physical microphone; μ_2 denotes the step size in the LMS algorithm; and $e_{p,m}(n)$ denotes the mth physical error signal.

In the control stage, the new control filter is computed as:

$$\begin{aligned}\mathbf{w}_{kj}(n+1) = \mathbf{w}_{kj}(n) - \mu_3 \sum_{m=1}^{M} \mathbf{x}'_{p,jkm}(n) \\ \times \left[e_{p,m}(n) - \mathbf{h}_{o,m}^T \mathbf{x}(n)\right],\end{aligned} \tag{4}$$

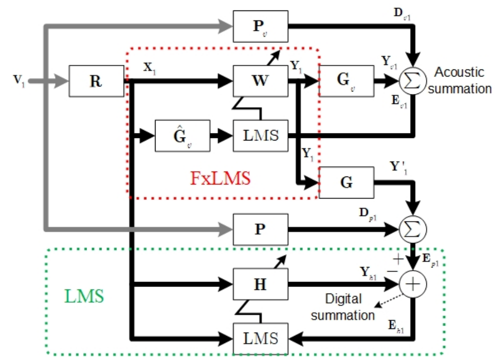

Fig. 2. Block diagram of VS-MCANC in the tuning stage (dotted box: digital processing block; rest: acoustic path).

where $x'_{p,jkm}(n)$ is the convolution of the jth reference signal $x_j(n)$ and the secondary path estimate $\hat{g}_{mk}(n)$, from the kth secondary source to the mth physical microphone; μ_3 denotes the step size in the control stage; and $\mathbf{h}_{o,m}$ represents the mth optimal auxiliary filter obtained from (3).

3. FREQUENCY DOMAIN ANALYSIS

In the multichannel active control of noise disturbances at the virtual microphone locations, error microphones must first be placed at these locations. The multichannel FxLMS algorithm used to minimize the sum-of-the-squared errors at these locations is shown in Fig. 2. The $(L \times 1)$ primary random noise vector $\mathbf{V}_1$ propagates through the $(J \times L)$ reference paths $\mathbf{R}$ to generate the $(J \times 1)$ reference vector $\mathbf{X}_1$. The error signal vector at the N virtual error microphone positions is given by

$$\mathbf{E}_{v1} = \mathbf{D}_{v1} + \mathbf{G}_v \mathbf{W} \mathbf{X}_1, \tag{5}$$

where $\mathbf{D}_{v1}$ is the $(N \times 1)$ vector of disturbances due to $\mathbf{V}_1$ propagating through the primary paths $\mathbf{P}_v$. $\mathbf{G}_v$ and $\mathbf{W}$ are the $(N \times K)$ secondary path and $(K \times J)$ control filter matrices, respectively. The power spectral density of the virtual error signal can be expressed as

$$J_{v1} = E\left[\mathbf{E}_{v1}^H \mathbf{E}_{v1}\right] = tr\left\{E\left[\mathbf{E}_{v1}\mathbf{E}_{v1}^H\right]\right\}, \tag{6}$$

where $E[\cdot]$ and $tr[\cdot]$ are the expectation and trace operators, respectively. By substituting (5) into (6) and using the properties of the trace operator, i.e., $tr[\mathbf{A}+\mathbf{B}] = tr[\mathbf{A}] + tr[\mathbf{B}]$ and $tr[\mathbf{AB}] = tr[\mathbf{BA}]$, we expand (6) to

$$\begin{aligned}J_{v1} = tr[\mathbf{S}_{d,v1} + \mathbf{W}^H \mathbf{G}_v^H \mathbf{S}_{xd,v1} + \mathbf{S}_{dx,v1} \mathbf{G}_v \mathbf{W} \\ + \mathbf{W}^H \mathbf{G}_v^H \mathbf{G}_v \mathbf{W} \mathbf{S}_{x1}],\end{aligned} \tag{7}$$

where the spectral density matrices for the reference and disturbance signals are $\mathbf{S}_{x1} = E[\mathbf{X}_1\mathbf{X}_1^H]$ and $\mathbf{S}_{d,v1} = E[\mathbf{D}_1\mathbf{D}_1^H]$, respectively. Their cross-spectral density matrix is defined as $\mathbf{S}_{xd,v1} = E[\mathbf{D}_{v1}\mathbf{X}_{v1}^H]$. The optimal control filter is calculated by minimizing the cost function in (7) by setting its gradient to zero

$$\nabla J_{v1} = 2\mathbf{S}_{xd,v1}^H \mathbf{G}_v + 2\mathbf{S}_{x1}^H \mathbf{W}_o^H \mathbf{G}_v^H \mathbf{G}_v = \mathbf{0}. \tag{8}$$

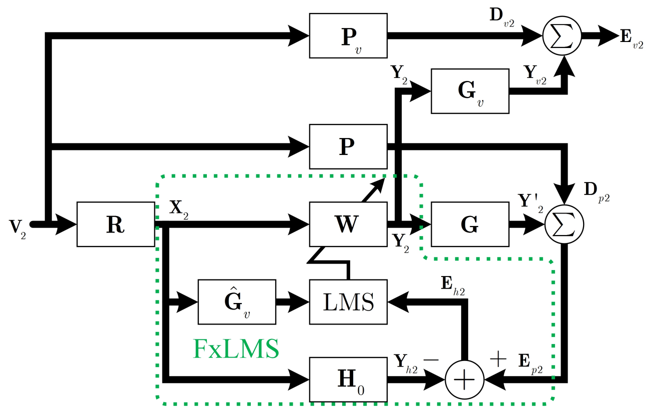

Fig. 3. Block diagram of VS-MCANC in the control stage.

Hence, the optimal control filter is derived as

$$\mathbf{W}_o = -\left[\mathbf{G}_v^H\mathbf{G}_v\right]^{-1}\mathbf{G}_v^H\mathbf{S}_{xd,v1}\mathbf{S}_{x1}^{-1}, \tag{9}$$

where $\mathbf{S}_{x1}$ is assumed to be invertible [14]. Since the disturbance and reference signals are respectively created by the passage of $\mathbf{V}_1$ through $\mathbf{P}_v$ and $\mathbf{R}$, $\mathbf{S}_{x1}$ and $\mathbf{S}_{d,v1}$ can be rewritten as $\mathbf{S}_{x1} = \mathbf{R}\mathbf{S}_{v1}\mathbf{R}^H$ and $\mathbf{S}_{xd,v1} = \mathbf{P}_v\mathbf{S}_{v1}\mathbf{R}^H$, where $\mathbf{S}_{v1} = E[\mathbf{V}_1\mathbf{V}_1^H]$. By inserting $[\mathbf{R}^H\mathbf{R}]^{-1}\mathbf{R}^H\mathbf{R} = \mathbf{I}$ into (9), the MCANC optimal control filter at the virtual error location can be rewritten as

$$\mathbf{W}_o = -\left[\mathbf{G}_v^H\mathbf{G}_v\right]^{-1}\mathbf{G}_v^H\mathbf{P}_v\left[\mathbf{R}^H\mathbf{R}\right]^{-1}\mathbf{R}^H. \tag{10}$$

In the second part of the tuning stage, the control filter in (10) is used to train the auxiliary filter, as shown in Fig. 2. Hence, the error signal vector used to update the auxiliary filter is given by

$$\mathbf{E}_{h1} = \mathbf{D}_{p1} + \mathbf{G}\mathbf{W}_o\mathbf{X}_1 - \mathbf{H}\mathbf{X}_1, \tag{11}$$

where $\mathbf{D}_{p1}$ and $\mathbf{G}$ are the vectors of disturbances and secondary path matrix to the physical error microphones, respectively; and $\mathbf{H}$ is the auxiliary filter matrix. The power spectral density of (11) is given by

$$J_{h1} = E\left[\mathbf{E}_{h1}^H\mathbf{E}_{h1}\right] = tr\left\{E\left[\mathbf{E}_{h1}\mathbf{E}_{h1}^H\right]\right\}. \tag{12}$$

Substituting (11) into (12) yields

$$\begin{aligned} J_{h1} = tr\{&\mathbf{S}_{d,p1} + \mathbf{S}_{xd,p1}\mathbf{W}_o^H\mathbf{G}^H - \mathbf{H}^H\mathbf{S}_{xd,p1} + \\ &\mathbf{G}\mathbf{W}_o\mathbf{S}_{dx,p1} + \mathbf{G}\mathbf{W}_o\mathbf{S}_{x1}\mathbf{W}_o^H\mathbf{G}^H - \mathbf{H}^H\mathbf{G}\mathbf{W}_o\mathbf{S}_{x1} \\ &- \mathbf{H}\mathbf{S}_{dx,p1} - \mathbf{H}\mathbf{S}_{x1}\mathbf{W}_o^H\mathbf{G}^H + \mathbf{H}^H\mathbf{H}\mathbf{S}_{x1}\}, \end{aligned} \tag{13}$$

where $\mathbf{S}_{xd,p1} = E[\mathbf{D}_{p1}\mathbf{X}_1^H] = \mathbf{P}\mathbf{S}_{v1}\mathbf{R}^H$, and $\mathbf{P}$ is the primary path to the physical error microphones. By setting the gradient of (13) to zero, we can derive the optimal auxiliary filter matrix as

$$\mathbf{H}_o = \left\{\mathbf{P} - \mathbf{G}\left[\mathbf{G}_v^H\mathbf{G}_v\right]^{-1}\mathbf{G}_v^H\mathbf{P}_v\right\}\left[\mathbf{R}^H\mathbf{R}\right]^{-1}\mathbf{R}. \tag{14}$$

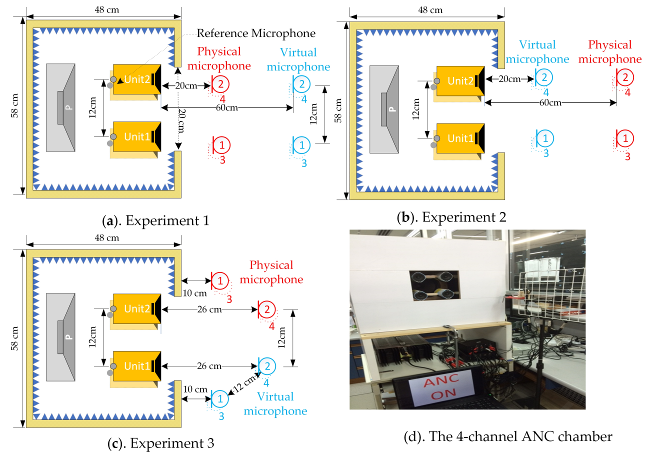

(a). Experiment 1
(b). Experiment 2
(c). Experiment 3
(d). The 4-channel ANC chamber

Fig. 4. The 4-channel VS-MCANC platform.

In the control stage, the actual microphones are removed from the virtual error locations, and the primary random noise vector is now $\mathbf{V}_2$, as shown in Fig. 3. The error signal vector $\mathbf{E}_h2$ used to update the control filter is given by

$$\mathbf{E}_{h2} = \mathbf{D}_{p2} + \mathbf{G}\mathbf{W}\mathbf{X}_2 - \mathbf{H}_o\mathbf{X}_2, \tag{15}$$

where $\mathbf{D}_{p2}$ and $\mathbf{X}_2$ are the vectors of disturbances at the physical error microphones and references, respectively. Hence, the power spectral density of (15) is given by

$$\begin{aligned} J_{h2} = tr\{&\mathbf{S}_{d,p2} + \mathbf{W}^H\mathbf{G}^H\mathbf{S}_{xd,p2} - \mathbf{S}_{xd,p2}\mathbf{H}_o^H + \\ &\mathbf{G}\mathbf{W}\mathbf{S}_{dx,p2} + \mathbf{W}^H\mathbf{G}^H\mathbf{G}\mathbf{W}\mathbf{S}_{x2} - \mathbf{G}\mathbf{W}\mathbf{S}_{x2}\mathbf{H}_o^H \\ &- \mathbf{H}_o\mathbf{S}_{dx,p2} - \mathbf{W}^H\mathbf{G}^H\mathbf{H}_o\mathbf{S}_{x2} + \mathbf{H}\mathbf{S}_{x2}\mathbf{H}_o^H\}, \end{aligned} \tag{16}$$

where $\mathbf{S}_{xd,p2} = \mathbf{P}\mathbf{S}_{v2}\mathbf{R}^H$, $\mathbf{S}_{x2} = \mathbf{R}\mathbf{S}_{v2}\mathbf{R}^H$, and $\mathbf{S}_{v2} = E[\mathbf{V}_2\mathbf{V}_2^H]$. The optimal control filter matrix is obtained by setting the gradient of (16) to zero as

$$\mathbf{W}_{o,c} = \left[\mathbf{G}^H\mathbf{G}\right]^{-1}\left(\mathbf{G}^H\mathbf{H}_o\mathbf{S}_{x2} - \mathbf{G}^H\mathbf{S}_{xd,p2}\right)\mathbf{S}_{x2}^{-1}, \tag{17}$$

where $\mathbf{S}_{xd,p2}$ is assumed invertible. By substituting (14) into (17), the optimal control filter in control stage is rewritten as

$$\mathbf{W}_{o,c} = -\left[\mathbf{G}_v^H\mathbf{G}_v\right]^{-1}\mathbf{G}_v^H\mathbf{P}_v\left[\mathbf{R}^H\mathbf{R}\right]^{-1}\mathbf{R}^H, \tag{18}$$

which is the same as the conventional MCANC with actual error microphones at the virtual locations. Hence, optimal control can be achieved at the desired virtual error microphone locations through the VS-MCANC algorithm. As shown in(17), the solution of control filter is composed of the auxiliary filter. However, in the formula (14) of the auxiliary filter, the transfer function of the virtual primary path is independent of the physical primary path. Hence, once getting the transfer functions of the microphones' paths, we can calculate the optimal auxiliary filter. Moreover, the final control filter of VS-MCANC in (18) does not require information about the secondary paths of physical error microphones. Therefore, the locations of the physical and virtual error microphones are independent in the VS-MCANC algorithm.

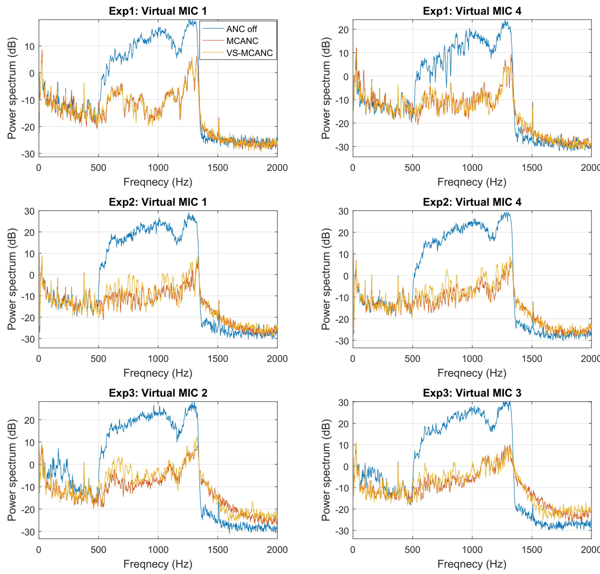

Fig. 5. Power spectrum of virtual error signal in three configurations.

4. REAL-TIME IMPLEMENTATION OF VS-MCANC

A 4-channel VS-MCANC algorithm was implemented in real time on a National Instruments PXI platform (NI PXIe 8880) with all filters at 512 taps and a fixed sample rate of 16 kHz. Four control sources, with information from four reference, physical and virtual microphones, were driven to control the broadband primary noise (500 Hz to 1.4 kHz) propagating through a square from the inside of a wooden chamber, as shown in Fig. 4. Three experimental configurations were investigated, as illustrated in Fig. 4 (a)-(c). In the first experiment shown in Fig. 4(a), the physical microphones were positioned closer to secondary sources than the virtual microphones. In the second experiment shown in Fig. 4(b), the locations of the physical and the virtual error microphones were swapped, such that the arrangements (transfer function from the physical microphone to the virtual microphone) were non-causal. Finally, the physical and virtual error microphones were symmetrically arranged such that there was no spatial correlation between both sets of microphones. In each experimental configuration, three algorithms were tested: (1) the conventional MCANC with virtual error microphones as the error microphones, (2) the VS-MCANC, and (3) the MCANC without VS by using only the physical error microphones.

The power spectrums of the error signals at the virtual microphone locations of the three experimental configurations are shown in Fig. 5. When ANC is activated, there is significant noise reduction at the virtual error microphone locations. Notably, both the VS-MCANC and the conventional MCANC exhibited similar power spectrum at the virtual error microphone locations. The attenuation levels at both the physical and virtual error microphone locations in all three experimental configurations and algorithms are shown in Fig.

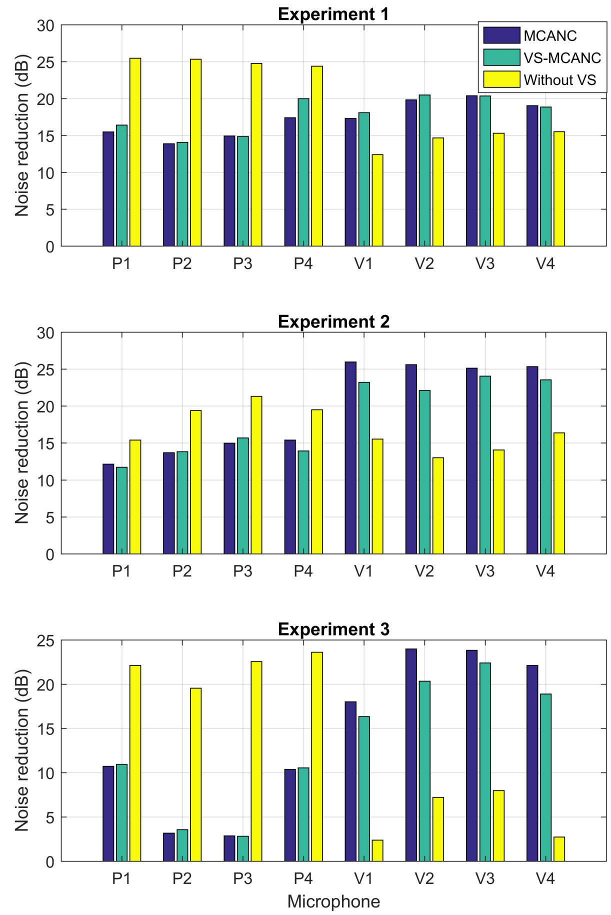

Fig. 6. Noise reduction at locations of error microphones.

6. The results indicate that both the VS-MCANC and the conventional MCANC have similar attenuation levels at the virtual microphone locations and both outperform the MCANC without VS technique. This experimental validation implies that the VS-MCANC algorithm can achieve the optimal noise control at the virtual error microphone locations without the spatial correlation and causality constraints.

5. CONCLUSION

Frequency domain analysis based on the control of random primary noise reveals that the proposed VS-MCANC algorithm could achieve the optimal noise reduction at the virtual error microphone locations. Compared to other multichannel VS-ANC techniques, the VS-MCANC uses the independent virtual and physical paths rather than the related information between the virtual and physical locations to update the control filter, which overcomes the spatial correlation and causality constraints between the physical and virtual microphones. Furthermore, a real-time 4-channel VS-MCANC was implemented to control broadband noise emitting from a test chamber, and its experimental results validate the theoretical analysis of the paper.

6. REFERENCES

[1] Yoshinobu Kajikawa, Woon-Seng Gan, and Sen M Kuo, "Recent advances on active noise control: open issues and innovative applications," *APSIPA Transactions on Signal and Information Processing*, vol. 1, 2012.

[2] Jordan Cheer, Stephen J Elliott, Eunmi Oh, and Jonghoon Jeong, "Application of the remote microphone method to active noise control in a mobile phone," *The Journal of the Acoustical Society of America*, vol. 143, no. 4, pp. 2142–2151, 2018.

[3] Rina Hasegawa, Yoshinobu Kajikawa, Cheng-Yuan Chang, and Sen M Kuo, "Headrest application of multi-channel feedback active noise control with virtual sensing technique," in *INTER-NOISE and NOISE-CON Congress and Conference Proceedings*. Institute of Noise Control Engineering, 2017, vol. 255, pp. 3513–3524.

[4] MRF Kidner, C Petersen, AC Zander, and CH Hansen, "Feasibility study of localised active noise control using an audio spotlight and virtual sensors," in *Proceedings of ACOUSTICS*, 2006, pp. 55–61.

[5] Xiaojun Qiu, "A review of near field acoustic error sensing strategies for active sound radiation control," in *Proceedings of of 25rd International Congress on Sound and Vibration*, 2018.

[6] J Garcia-Bonito, SJ Elliott, and CC Boucher, "Generation of zones of quiet using a virtual microphone arrangement," *The journal of the Acoustical Society of America*, vol. 101, no. 6, pp. 3498–3516, 1997.

[7] Jacqueline M Munn, Ben S Cazzolato, Colin D Kestell, and Colin H Hansen, "Virtual error sensing for active noise control in a one-dimensional waveguide: Performance prediction versus measurement (l)," *The Journal of the Acoustical Society of America*, vol. 113, no. 1, pp. 35–38, 2003.

[8] Colin D Kestell, Ben S Cazzolato, and Colin H Hansen, "Active noise control in a free field with virtual sensors," *The Journal of the Acoustical Society of America*, vol. 109, no. 1, pp. 232–243, 2001.

[9] Lichuan Liu, Sen M Kuo, and MengChu Zhou, "Virtual sensing techniques and their applications," in *Networking, Sensing and Control, 2009. ICNSC'09. International Conference on*. IEEE, 2009, pp. 31–36.

[10] Shoma Edamoto, Chuang Shi, and Yoshinobu Kajikawa, "Virtual sensing technique for feedforward active noise control," in *Proceedings of Meetings on Acoustics 172ASA*. ASA, 2016, vol. 29, p. 030001.

[11] Stephen J Elliott, Woomin Jung, and Jordan Cheer, "Head tracking extends local active control of broadband sound to higher frequencies," *Scientific reports*, vol. 8, no. 1, pp. 5403, 2018.

[12] Danielle Moreau, Ben Cazzolato, Anthony Zander, and Cornelis Petersen, "A review of virtual sensing algorithms for active noise control," *Algorithms*, vol. 1, no. 2, pp. 69–99, 2008.

[13] Marek Pawelczyk, "Feedback control of acoustic noise at desired locations," *Silesian University of Technology, Gliwice*, 2005.

[14] Stephen J Elliott and Jordan Cheer, "Modeling local active sound control with remote sensors in spatially random pressure fields," *The Journal of the acoustical Society of america*, vol. 137, no. 4, pp. 1936–1946, 2015.

[15] Debi Prasad Das, Danielle J Moreau, and Ben S Cazzolato, "A nonlinear active noise control algorithm for virtual microphones controlling chaotic noise," *The Journal of the Acoustical Society of America*, vol. 132, no. 2, pp. 779–788, 2012.

[16] Cornelis D Petersen, Rufus Fraanje, Ben S Cazzolato, Anthony C Zander, and Colin H Hansen, "A kalman filter approach to virtual sensing for active noise control," *Mechanical Systems and Signal Processing*, vol. 22, no. 2, pp. 490–508, 2008.

[17] Woomin Jung, Stephen J Elliott, and Jordan Cheer, "Combining the remote microphone technique with head-tracking for local active sound control," *The Journal of the Acoustical Society of America*, vol. 142, no. 1, pp. 298–307, 2017.

[18] Marek Pawelczyk, "Adaptive noise control algorithms for active headrest system," *Control Engineering Practice*, vol. 12, no. 9, pp. 1101–1112, 2004.

[19] Nobuhiro Miyazaki and Yoshinobu Kajikawa, "Head-mounted active noise control system with virtual sensing technique," *Journal of Sound and Vibration*, vol. 339, pp. 65–83, 2015.

[20] Nobuhiro Miyazaki and Yoshinobu Kajikawa, "Adaptive feedback anc system using virtual microphones," in *Acoustics, Speech and Signal Processing (ICASSP), 2013 IEEE International Conference on*. IEEE, 2013, pp. 383–387.

[21] Reo Maeda, Yoshinobu Kajikawa, Cheng-Yuan Chang, and Sen Maw Kuo, "Helmet anc system with virtual sensing technique," in *Proceedings of of 25rd International Congress on Sound and Vibration*, 2018.